Heliyon 9 (2023) e21997

Contents lists available at ScienceDirect

Heliyon

journal homepage: www.cell.com/heliyon

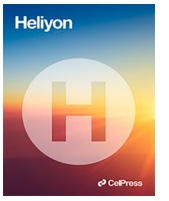

The mechanism of Shenbing Decoction II against IgA nephropathy renal fibrosis revealed by UPLC-MS/MS, network pharmacology and experimental verification

Huaxi Liu [a,1], Weijie Chen [a,1], Chunyang Tian [a,1], Yijian Deng [a], Liangwo Xu [a], Wenkun Ouyang [a], Renjie Qiu [a], Yanting You [a], Pingping Jiang [a], Lin Zhou [b], Jingru Cheng [c], Hiu Yee Kwan [d], Xiaoshan Zhao [a,**], Xiaomin Sun [a,*]

[a] *Syndrome Laboratory of Integrated Chinese and Western Medicine, School of Chinese Medicine, Southern Medical University, Guangzhou, Guangdong, China*
[b] *Endocrinology Department, Nanfang Hospital, Southern Medical University, Guangzhou, Guangdong, China*
[c] *Department of Nephrology, the First Affiliated Hospital of Zhengzhou University, Zhengzhou, Henan, China*
[d] *School of Chinese Medicine, Hong Kong Baptist University, Hong Kong, China*

A R T I C L E I N F O

Keywords:
Shenbing Decoction II
IgA nephropathy
Renal fibrosis
Network pharmacology
TP53
PI3K-Akt signaling pathway

A B S T R A C T

Background: IgA nephropathy (IgAN) is a major and growing public health problem. Renal fibrosis plays a vital role in the progression of IgAN. This study is to investigate the mechanisms of action underlying the therapeutic effects of Shenbing Decoction II (SBDII) in IgAN renal fibrosis treatment based on ultra-performance liquid chromatography-tandem mass spectrometry (UPLC-MS/MS), network pharmacology and experimental verification.

Method: We first used UPLC-MS/MS to explore the main compounds of SBDII, and then used network pharmacology to predict the targets and key pathways of SBDII in the treatment of IgAN renal fibrosis. Next, bovine serum albumin (BSA), lipopolysaccharide (LPS), and carbon tetrachloride (CCL4) were used to induce IgAN in rats, and then biochemical indicators, renal tissue pathology, and renal fibrosis-related indicators were examined. At the same time, part of the results predicted by network pharmacology were also verified.

Result: A total of 105 compounds were identified in SBDII by UPLC-MS/MS. Network pharmacology results showed that the active compounds such as acacetin, eupatilin, and galangin may mediate the therapeutic effects of SBDII in treating IgAN by targeting tumor protein p53 (TP53) and regulating phosphatidylinositol 3-kinase (PI3K)-Akt kinase (Akt) signaling pathway. Animal experiments showed that SBDII not only significantly improved renal function and fibrosis in IgAN rats, but also significantly downregulated the expressions of p53, p-PI3K and *p*-Akt.

Conclusion: This UPLC-MS/MS, network pharmacological and experimental study highlights that the TP53 as a target, and PI3K-Akt signaling pathway are the potential mechanism by which SBDII is involved in IgAN renal fibrosis treatment. Acacetin, eupatilin, and galangin are probable

* Corresponding author. Syndrome Laboratory of Integrated Chinese and Western Medicine, School of Chinese Medicine, Southern Medical University, Guangzhou, Guangdong, 510515, China.
** Corresponding author. Syndrome Laboratory of Integrated Chinese and Western Medicine, School of Chinese Medicine, Southern Medical University, Guangzhou, Guangdong, 510515, China.
E-mail addresses: zhaoxs0609@163.com (X. Zhao), sunxiaomin198001@163.com (X. Sun).
[1] These authors contributed equally to this work.

https://doi.org/10.1016/j.heliyon.2023.e21997
Received 30 March 2023; Received in revised form 31 October 2023; Accepted 1 November 2023
Available online 3 November 2023

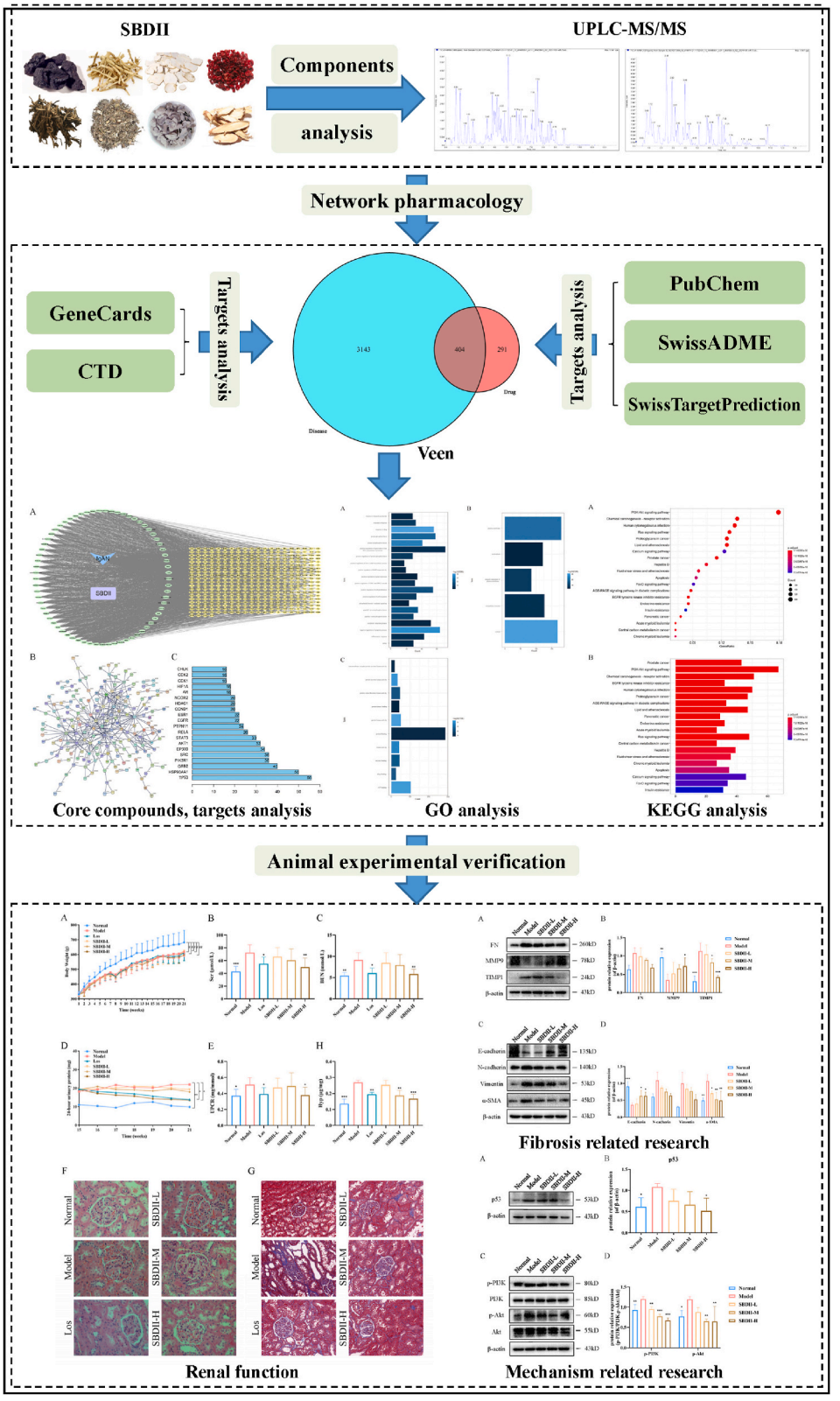

Fig. 1. The technical strategy of the current study.

active compounds in SBDII, these results might provide valuable guidance for further studies of IgAN renal fibrosis treatment.

1. Introduction

IgA nephropathy (IgAN) is a primary glomerular disease characterized by IgA deposition alone or coexisting with IgG and IgM in the mesangial region, and is also one of the main causes of end-stage renal failure (ESRF). Renal fibrosis plays a vital role in the progression of IgAN to ESRF [1]. The main manifestations of renal fibrosis include glomerulosclerosis and renal interstitial fibrosis (RIF) [2]. The imbalance of glomerular extracellular matrix (ECM) synthesis and degradation plays an important role in the process of glomerulosclerosis, and the renal tubular epithelial cell epithelial-mesenchymal transition (EMT) is considered one of the most important sources of myofibroblasts and an important mechanism of RIF. Epidemiological studies show that IgAN has a global prevalence of 2.5 cases per 100,000 adults per year [3], and a study in Asia shows that approximately 30 % of patients with IgAN will develop ESRF within 30 years [4]. Therefore, the prevalence should be prevented.

Due to the lack of specific treatment, renal fibrosis of IgAN can only be treated by western medicine symptomatically, and some of the drugs have side effects. Glucocorticoids and immunosuppressants are commonly used to control proteinuria [5]. Traditional Chinese medicine (TCM) has unique advantages and characteristics in the prevention and treatment of renal fibrosis in IgAN. Shenbing Decoction II (SBDII) is a TCM formula with significant curative effect as summarized by our research group based on many years of clinical experience [6]. This decoction comprises eight medicinal herbs and has the effects of nourishing kidney and filling essence, clearing heat and cooling blood. Our previous randomized controlled studies found that SBDII can treat IgAN by targeting anti-oxidative stress and improving the immune function of red blood cells without undesired toxicity and side-effects [7–9]. However, there is no further study on its active compounds and its therapeutic mechanisms. The current research methods have limitations in obtaining a comprehensive picture of its network action mechanisms.

UPLC-MS/MS is a new technology emerging in recent years, which meets the demand of automated and high-throughput research methods in modern TCM compounds, and has become one of the important methods for the identification and analysis of TCM compounds. Network pharmacology is a new idea for drug design based on network biology and multidirectional pharmacology. It is a holistic and systematic approach and is compatible with the complex system of TCM with multi-component, multi-pathway, and multi-target properties [10–14]. The application of network pharmacology in recent years has provided new ideas and perspectives for the in-depth study of large and complex TCM systems for treating diseases.

In this study, the components of SBDII were first analyzed by UPLC-MS/MS, and then network pharmacology was used to investigate the active compounds, targets, and mechanisms of SBDII in treating IgAN renal fibrosis, and animal experiments were also conducted to validate the potential mechanism of SBDII on IgAN renal fibrosis, as predicted by network pharmacology approach. The detailed technical strategy of the current study was shown in Fig. 1.

2. Materials and methods

2.1. Standard production process of SBDII

SBDII was derived from eight herbs, *Rehmannia glutinosa* (Gaertn.) DC., *Dioscorea japonica* Thunb., *Ostrea gigas* Thunberg, *Cornus officinalis* Siebold & Zucc., *Imperata cylindrica* (L.) Raeusch., *Cirsium japonicum* (Thunb.) Fisch. ex DC., *Cirsium arvense* (L.) Scop., *Glycyrrhiza glabra* L. All herbs were purchased from Pharmacy of TCM, Nanfang Hospital, Southern Medical University. The above mentioned 8 herbs were mixed at a ratio of 2:3:3:2:3:2:2:0.5 by weight. The mixture was boiled in 4 times ultrapure water in a Chinese medicine decocting pot for 2 h, and the obtained decoction was put into another container. Then, the above-mentioned mixture was kept boiling for 1.5 h in 2 vol of ultrapure water. The decoction was then filtered by a filter cloth and concentrated in a rotary evaporator (Shanghai Renhe Scientific Instrument Co., Ltd., Shanghai, China). The prepared decoction was frozen at −80 °C for storage.

2.2. Analysis of the major components in the SBDII

The samples were put into vacuum freeze-drying machine, and ground to powder at 30Hz and 90s by grinder. Weigh 100 mg powder and dissolve in 1.2 mL 70 % methanol, vortex once every 30min for 30s each time, vortex 6 times, after the end of the sample in 4 °C refrigerator overnight. And then centrifuged at 12000 rpm for 10 min. The supernatant was filtered through 0.22 μm filter and filter-through liquid was used for subsequent analysis.

The following liquid phase conditions were applied. Column: SB-C18 1.8 μm 2.1 × 100 mm, Agilent. Mobile phase A: ultrapure water (adding 0.1 % formic acid). Mobile phase B: acetonitrile (adding 0.1 % formic acid). Elution gradient: 0–9min, the proportion of mobile phase B increased linearly from 5 % to 95 %, and maintained at 95 % for 1min; 10–11min, the proportion of mobile phase B decreased to 5 %, and was balanced at 5 % to 14min. Flow rate: 0.35 mL/min. Column temperature: 40 °C. Injection volume: 4 μL.

The mass spectrometry conditions were as follows. Ion source: turbo spray. Source temperature: 550 °C. Ion spray voltage (positive ion mode): 5500V; ion spray voltage (negative ion mode): 4500V. The ion source gas I, gas II, and curtain gas were set to 50, 60, and 25psi, respectively, and the collision-induced ionization parameter was set to be high.

2.3. Network pharmacology analysis

The 2D structures of the major components of SBDII were downloaded from PubChem database (https://pubchem.ncbi.nlm.nih.gov/) in. sdf format, and then the SwissADME online platform (http://www.swissadme.ch/index.php#) was used to screen and remove the components with poor gastrointestinal absorption (GI absorption as Low). The SwissTargetPrediction platform (http://www.swisstargetprediction.ch/) was employed to predict the potential targets for eligible components. Enter "IgA nephropathy" and "renal fibrosis" in the search box of the GeneCards database (https://www.genecards.org/) and CTD database (http://ctdbase.org/), respectively, to find the same targets as the targets related to SBDII in all displayed target results. The active molecule-target interaction network was generated in Cytoscape 3.7.2 software. A target PPI network was constructed in the STRING database (https://cn.string-db.org/) with a confidence level of 0.99. For GO enrichment analysis, the DAVID 6.8 database (https://david.ncifcrf.gov/) was used. And the R package clusterProfiler in Bioconductor was used for KEGG pathway enrichment analysis.

2.4. Animal experimental design

Forty SPF 4-week-old male Sprague-Dawley (SD) rats weighing 180–220g were bought from Experimental Animal Center of Guangdong Province. SD rats were randomly divided into six groups (n = 8/group), including normal group, model group, Losartan (Los) group, low dose SBDII (SBDII-L) group, medium dose SBDII (SBDII-M) group and high dose SBDII (SBDII-H) group. The IgAN experimental animal model was established by treatment with bovine serum albumin (BSA, Sigma-Aldrich, USA), lipopolysaccharide (LPS, Sigma-Aldrich, USA), and carbon tetrachloride (CCL4, Aladdin, Shanghai, China) [15–17], and specific implementation was as follows: BSA (600 mg/kg, gavage every other day), CCL4 (0.1 mL, plus 0.5 mL castor oil, subcutaneous injection once a week) and LPS (0.25 mg/kg, caudal vein injection at week 7, 10 and 13) for 14 weeks. The dosage of herbs were calculated based on the body surface area. The dosage of SBDII-M group was equivalent to the clinical single-day dosage, and the SBDII-H group and SBDII-L group dose corresponded to 2 and 0.5 times of the SBDII-M group dose. Rats of SBDII-L group, SBDII-M group, and SBDII-H group were given SBDII doses of 8 g/kg/d (SBDII-L), 16 g/kg/d (SBDII-M) and 32 g/kg/d (SBDII-H) by daily gavage starting from week 15 until week 20. Losartan (30 mg/kg/d) was used as western medicine control in this study [18,19]. Rats of the normal group and model group were given the same amount (10 mL/kg) of purified water by daily gavage.

The body weights of the rats were recorded weekly during the experiment. Starting from week 15, urine was collected weekly from each rat for 24 h. The day before sacrifice, a morning spot urine sample was collected for measurement of urine protein-to-creatinine ratio (UPCR). At the end of the experimental period, blood samples were collected from the aorta and then kept at room temperature for 30 min, and the blood was centrifuged at 4 °C and 3500 rpm in a TOMY RS-20 centrifuge (TOMY SEIKO, Tokyo, Japan) for 10 min. Serum samples and right kidney were stored at −80 °C until assay. The left kidney tissues were fixed in 4 % paraformaldehyde until further use.

2.5. Biochemical assays

Serum creatinine (Scr), blood urea nitrogen (BUN), and urine protein levels were detected using various kits. The assay procedures were following the kit instructions (Jiancheng Biology Institution, China).

2.6. Renal pathology

Kidney tissues were fixed in 4 % paraformaldehyde, embedded in paraffin, and cut into 4 μm sections. The kidney histopathological changes were observed under a light microscope after hematoxylin and eosin (H&E) stains. Masson staining was performed using standard methods to observe collagen fiber deposition in kidney tissues.

2.7. Hydroxyproline assays

Hydroxyproline (Hyp) content in kidney tissues was conducted using the alkali hydrolysis method. The assay procedures were following the kit instructions (Jiancheng Biology Institution, China).

2.8. Western blot

The antibodies against fibronectin (FN), matrix metallopeptidase 9 (MMP9), TIMP metallopeptidase inhibitor 1 (TIMP1), Vimentin, α-smooth muscle actin (α-SMA), p53, p-PI3K, PI3K, *p*-Akt, Akt, and β-actin were purchased from Affinity Biosciences (United States). E-cadherin and N-cadherin were purchased from Cell Signaling Technology (Danvers, MA, United States). For western blotting, tissue homogenates were used for protein extraction in RIPA lysis buffer. Proteins were quantified using the BCA kit (Thermo Fisher Scientifific, Inc.). After electrophoresis and membrane transferring, the membranes were blocked for 2 h in 5 % non-fat milk and then incubated at 4 °C overnight with anti-FN (1:500), anti-MMP9 (1:500), anti-TIMP1 (1:500), anti-E-cadherin (1:1000), anti-N-cadherin (1:1000), anti-Vimentin (1:500), anti-α-SMA (1:500), anti-p53 (1:500), anti-p-PI3K (1:500), anti-PI3K (1:500), anti-*p*-Akt (1:500), anti-Akt (1:500) and anti-β-actin (1:3000). Secondary antibody (Thermo Fisher Scientifific, Inc., 1:1000) was then applied for 2 h incubation at 4 °C, followed by development and exposure.

2.9. Statistical analysis

The experimental data were shown by mean ± SD. One-Way ANOVA was used for comparison between multiple groups, and then LSD test (when the variance is uniform) or Dunnett 's T3 test (when the variance is uneven) was used. Results were considered statistically significant at a level of $P < 0.05$. SPSS 26.0 and GraphPad Prism 8.0 software were used for statistics and graphing.

3. Results

3.1. The major components of SBDII

Supplementary Fig. 1 shows the 8 herbs that make up SBDII. A total of 105 compounds were identified in SBDII (Fig. 2A and B, Supplementary Table 1). They were assigned to 9 compound classes, including flavonoids, phenolic acids, amino acids and derivatives, organic acids, alkaloids, terpenoids, nucleotides and derivatives, lignans and coumarins, and other compounds including sugars, alcohols and vitamins. Among them, flavonoids and phenolic acids accounted for the highest proportion in SBDII, 37.1 % and 20.0 %, respectively.

3.2. Network pharmacology analysis for SBDII

We collected 695 potential targets of active molecules of SBDII in SwissTargetPrediction and retrieved 3547 targets related to IgAN renal fibrosis in the GeneCards and CTD databases. A total of 404 matching targets of the related targets of drugs and disease were collected as potential targets of SBDII on IgAN renal fibrosis (Fig. 3, Supplementary Table 2).

After removing active molecules that had no molecular targets, the active molecule-target interaction network was constructed using Cytoscape 3.7.2 software. It can be seen from Fig. 4A that SBDII played a therapeutic role in IgAN renal fibrosis through multicomponent and multitarget. With further analysis of this network, we found that this network included a total of 475 nodes (1 disease, 1 drug, 69 compounds, and 404 potential targets) and 2806 edges, and acacetin, eupatilin, and galangin had the greatest number of potential targets of 76, followed by hispidulin, apigenin, licochalcone E, licoisoflavanone each with 75, 74, 74, 73. In addition, quercetin, diosmetin, glyasperin D, liquiritigenin, naringenin also have multiple molecular targets, which indicate that the above-mentioned active molecules may be the key components of SBDII in the treatment of IgAN renal fibrosis. The UPLC-MS/MS graphs of these compounds are shown in Supplementary Fig. 2A-L. Next, the STRING database was used to obtain target protein interactions for potential targets. According to Fig. 4B and C, the eight targets that had the highest degree among the 404 potential targets are tumor protein p53 (TP53), heat shock protein 90 alpha family class A member 1 (HSP90AA1), growth factor receptor bound protein 2 (GRB2), phosphoinositide-3-kinase regulatory subunit 1 (PIK3R1), SRC proto-oncogene, non-receptor tyrosine kinase (SRC), E1A binding protein p300 (EP300), AKT serine/threonine kinase 1 (AKT1) and signal transducer and activator of transcription 3 (STAT3). These eight targets are the core targets for SBDII treatment of IgAN renal fibrosis.

The DAVID database was used to perform GO enrichment analysis on 404 potential targets. After sorting the analysis results by FDR values, it was found that these targets are mainly involved in biological processes (BP) such as response to drugs, negative regulation of apoptotic process, protein autophosphorylation, protein phosphorylation, peptidyl-tyrosine phosphorylation, and primarily distributed in cellular components (CC) such as cytosol, plasma membrane, integral component of plasma membrane, extracellular exosome, nucleoplasm, and mainly concentrated in molecular functions (MF) such as protein kinase activity, ATP binding, protein tyrosine kinase activity, kinase activity, enzyme binding (Fig. 5A–C). In addition, we also used the R package clusterProfiler in Bioconductor to perform KEGG pathway enrichment analysis of these targets, and found that PI3K-Akt signaling pathway was the most closely related to SBDII for IgAN renal fibrosis (Fig. 6A and B).

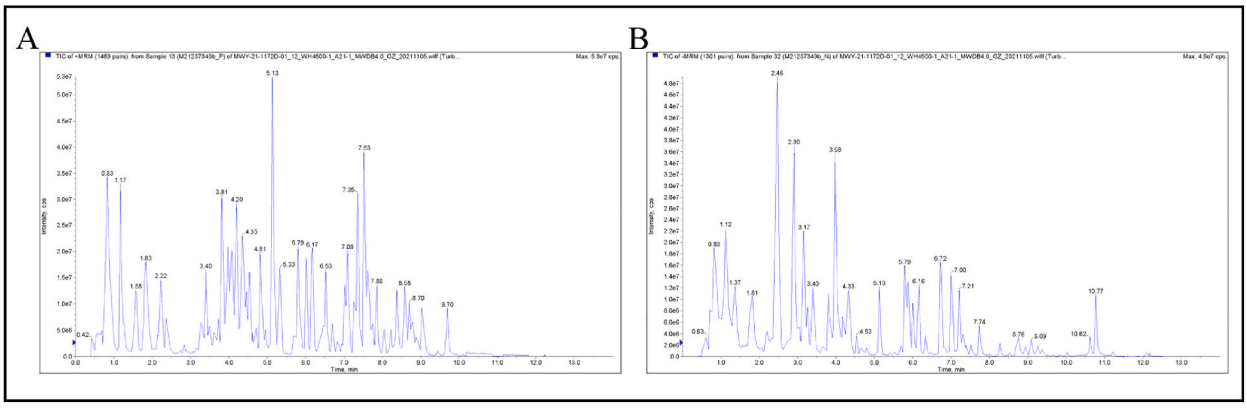

Fig. 2. Total ion chromatography of SBDII. (A) Total ion chromatography of SBDII in positive ion mode. **(B)** Total ion chromatography of SBDII in negative ion mode.

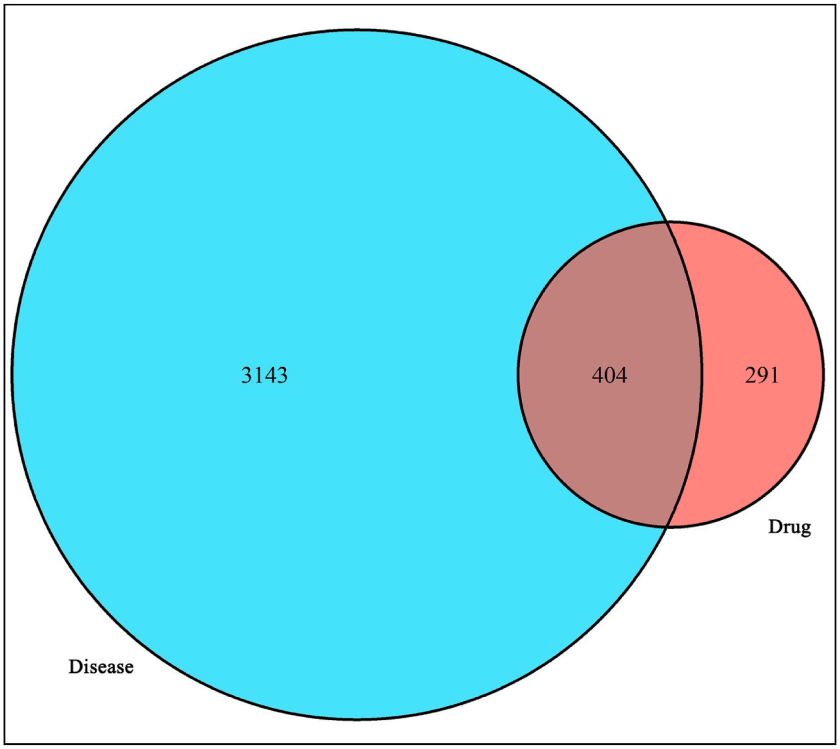

Fig. 3. The venn diagram of the targets both in SBDII targets and IgAN renal fibrosis targets.

3.3. SBDII improves renal function and abnormal pathological changes in renal tissue in IgAN rats

In this study, the rats with IgAN developed significant weight loss. Scr, BUN, 24-h urinary protein, and UPCR in the model group were increased compared to the normal group, which suggested renal insufficiency in these rats. Treatment with losartan and different doses of SBDII showed some protective effect on the renal function and with the most potent effect at higher doses, but the treatment could not restore the weight gain in these rats (Fig. 7A–E). Consistent with biochemical markers, H&E staining showed that the glomerular mesangial cells had mild or moderate proliferation, matrix accumulation, glomerular basement membrane thickening, and some renal tubular epithelial cells swelling in IgAN rats. In stark contrast, the glomerular and tubular lesions of rats treated with SBDII-H were alleviated, while the effect of Los was not as potent as SBDII-H (Fig. 7F). Masson staining and Hyp assay revealed that SBDII-M, SBDII-H and losartan improved collagen deposition in IgAN rats, especially SBDII-H (Fig. 7G and H).

In addition, we found no significant differences in serum AST and ALT levels and liver histopathology between the treatment groups and the control group, suggesting that SBDII is free of side effects (Supplementary Figs. 3A–C).

3.4. SBDII improves renal fibrosis in IgAN rats through targeting TP53 and regulating PI3K-Akt pathway

To determine whether the kidneys of rats with IgAN have fibrosis, Western blot was used to test the glomerulosclerosis and RIF markers in the kidney samples. As expected, the protein level of MMP9 was lower in the renal tissue of IgAN rats, whereas the protein level of TIMP1 was higher in this model compared with their controls, and although not statistically significant, the protein level of FN was also elevated in the model, indicating glomerulosclerosis. Similarly, the protein expression of E-cadherin was significantly reduced and α-SMA protein expression level was significant increased in the model group when compared with the normal group, and although not statistically significant, the protein levels of N-cadherin and Vimentin were also elevated in the model, which indicated RIF. These protein changes were reversed to varying degrees after different dosages of SBDII treatment, with SBDII-H exhibiting the most prominent effects (Fig. 8A–D). Besides, we verified the key target and the core signaling pathway predicted by network pharmacology and found that SBDII reversed the increased expressions of p53, p-PI3K and *p*-Akt protein in the kidney tissues of IgAN rats (Fig. 9A–D). Taken together, these findings suggest that SBDII-H significantly improves renal fibrosis in rats with IgAN through targeting TP53 and regulating PI3K-Akt pathway.

4. Discussion

IgAN belongs to the category of “hematuria”, “edema” in TCM. Its pathogenesis is a deficiency in origin and excess in superficiality, and its disease location is in the lung, spleen, liver, and kidney. After observation and analysis of a large number of clinical cases, and

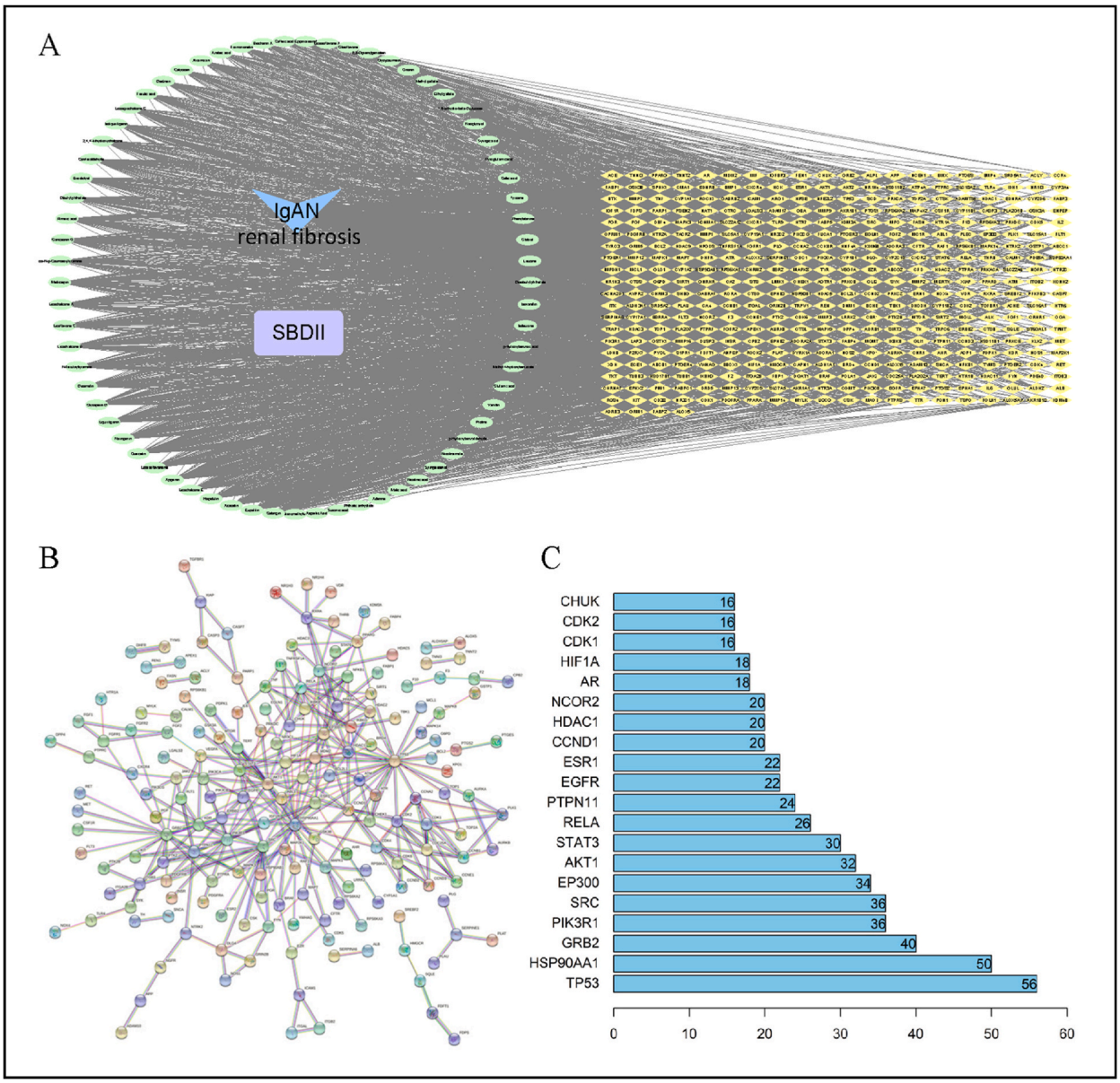

Fig. 4. Core compounds, targets analysis of SBDII for IgAN renal fibrosis. (A) Active molecule-target network, purple node represents SBDII, green nodes represent active molecules, yellow nodes represent potential targets, blue node represents IgAN renal fibrosis. **(B)** PPI network of potential targets, minimum required interaction score is 0.99, the contents of nodes are the 3D structures of targets, the edges represent the interaction between the targets (light blue: from curated databases; magenta: experimentally determined; green: gene neighborhood; red: gene fusions; blue: gene co-occurrence; yellow: textmining; black: co-expression; purple: protein homology). **(C)** Core targets in PPI network, the top 20 terms are shown.

combined with the theory of syndrome differentiation and treatment in TCM, our research group concluded SBDII for the treatment of IgAN. In the prescription, *Rehmannia glutinosa* (Gaertn.) DC. nourishes the yin and nourishes the kidney, fills the essence and nourishes the marrow, and is the main drug for nourishing the kidney yin; *Imperata cylindrica* (L.) Raeusch. cools blood to stop bleeding, clears heat and diuresis. The famous TCM expert Xichun Zhang believes that "*Rehmannia glutinosa* (Gaertn.) DC.-*Imperata cylindrica* (L.) Raeusch." are one warm and the other cool, one supplement and the other clear. They restrict and influence each other and are often used as a medicine pair. In SBDII, the two are used together to nourish yin and cool blood to stop bleeding, and the dose of the medicine pair is nearly one-third of the total dose of the whole prescription, so they are both regarded as monarch drugs. *Dioscorea japonica* Thunb. nourishes the spleen and kidney, and strengthens the kidney; *Cornus officinalis* Siebold & Zucc. nourishes the liver and kidney, but also obscures essence; *Cirsium japonicum* (Thunb.) Fisch. ex DC. and *Cirsium arvense* (L.) Scop. cool blood to stop bleeding, disperse blood stasis and diuresis, the four drugs are shared as minister drugs. *Ostrea gigas* Thunberg constricts yin and solidifies astringent,

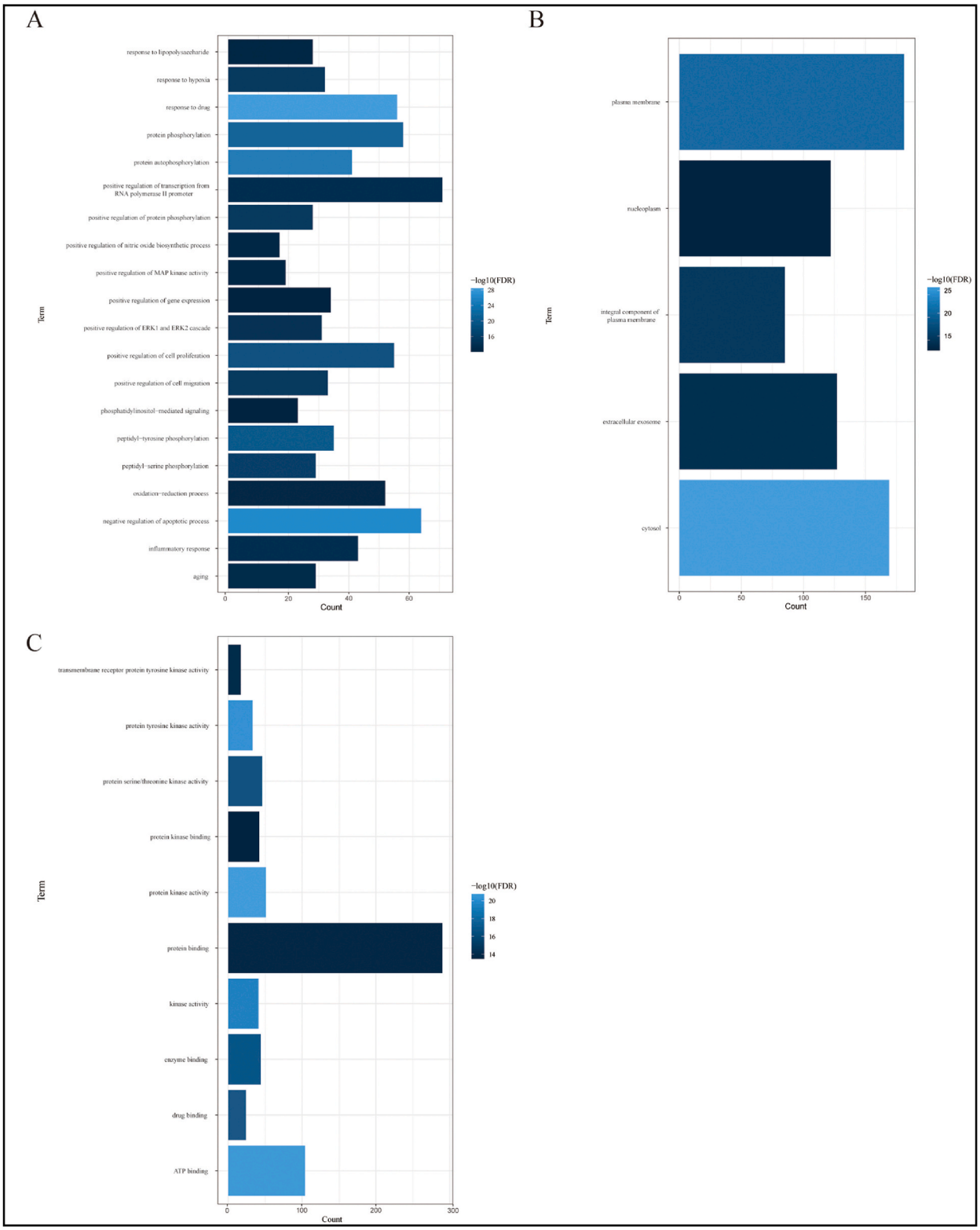

Fig. 5. GO enrichment analysis of potential targets. (A) The top 20 terms with FDR<0.05 are shown in BP. **(B)** The top 5 terms with FDR<0.05 are shown in CC. **(C)** The top 10 terms with FDR<0.05 are shown in MF.

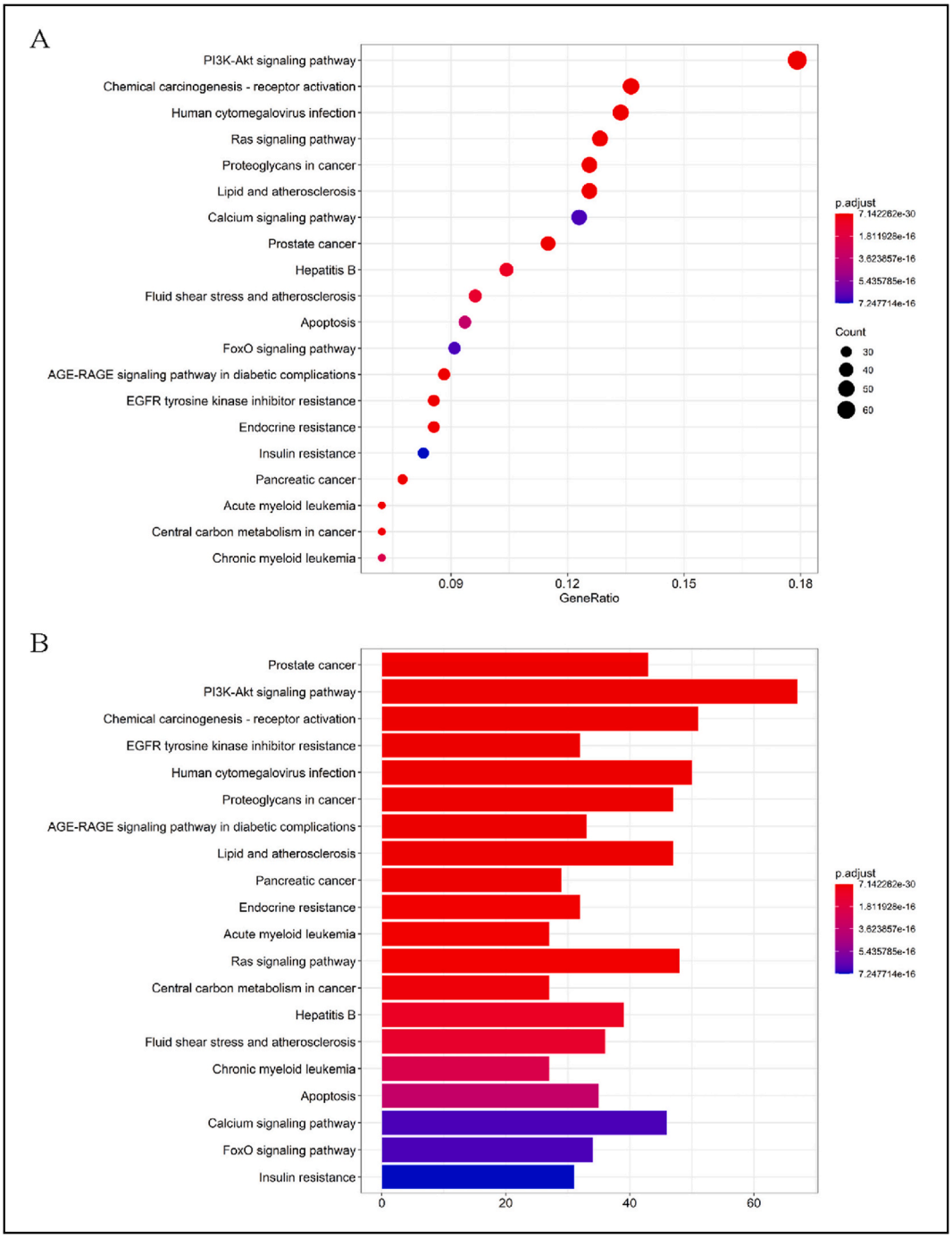

Fig. 6. KEGG pathway enrichment analysis of potential targets. (A) The top 20 terms with the most targets are shown. The larger the bubble, the more the potential targets are contained in this pathway; the closer the bubble color is to red, the smaller the *P* value. **(B)** The top 20 terms with the smallest *P* value are shown. The closer the bar color is to red, the smaller the *P* value.

Glycyrrhiza glabra L. reconciles various drugs, they are deemed as assistant drug and guide drug respectively. Modern pharmacological research results showed that "*Rehmannia glutinosa* (Gaertn.) DC.-*Imperata cylindrica* (L.) Raeusch." can treat IgAN by regulating the VEGF signaling pathway [20]. In addition, *Dioscorea japonica* Thunb., *Cornus officinalis* Siebold & Zucc., *Cirsium japonicum* (Thunb.) Fisch. ex DC., *Cirsium arvense* (L.) Scop., and *Glycyrrhiza glabra* L. were also proven to be common and effective Chinese medicines for the treatment of IgAN through data mining [21].

This study used network pharmacology to predict that there are 695 targets of active molecules for SBDII, 58.1 % of which are

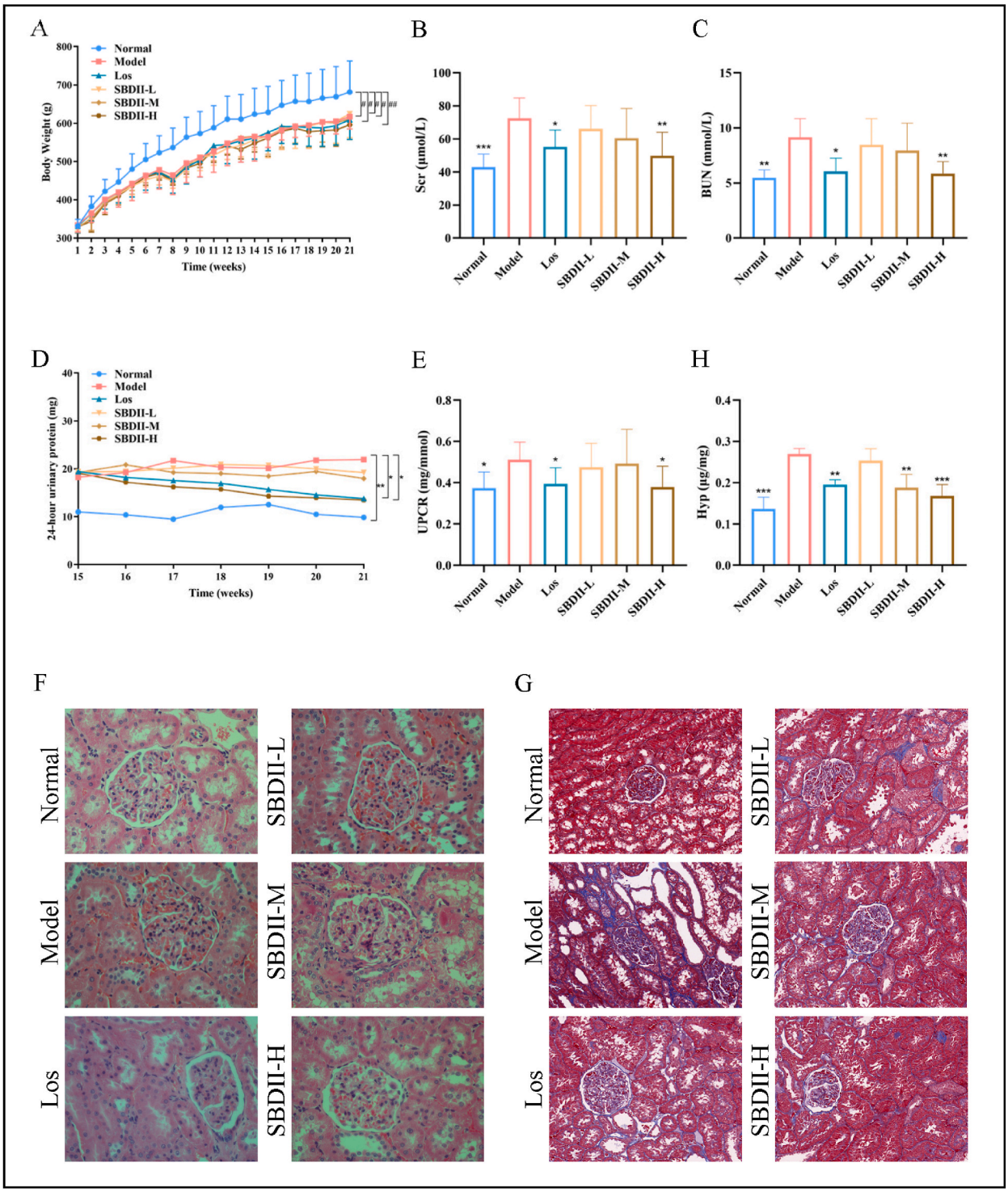

Fig. 7. SBDII treatment improves renal function and abnormal pathological changes in renal tissue in rats with IgAN. (A). Changes in rats body weight during the treatment. **(B-C)** Scr and BUN levels in rats at the end of the experiment. **(D)** Changes of 24-hour urinary protein in rats during treatment. **(E)** UPCR level in rats at the end of the experiment. **(F)** Representative images of renal histopathological findings in rats at the end of the experiment (H&E staining, 400x). **(G)** Representative images of renal histopathological findings in rats at the end of the experiment (Masson staining, 200x). **(H)** Hyp content in kidney tissues in rats at the end of the experiment. Data are expressed as the mean±SD. # $P<0.05$ (versus normal group). * $P<0.05$, ** $P<0.01$, *** $P<0.001$ (versus model group).

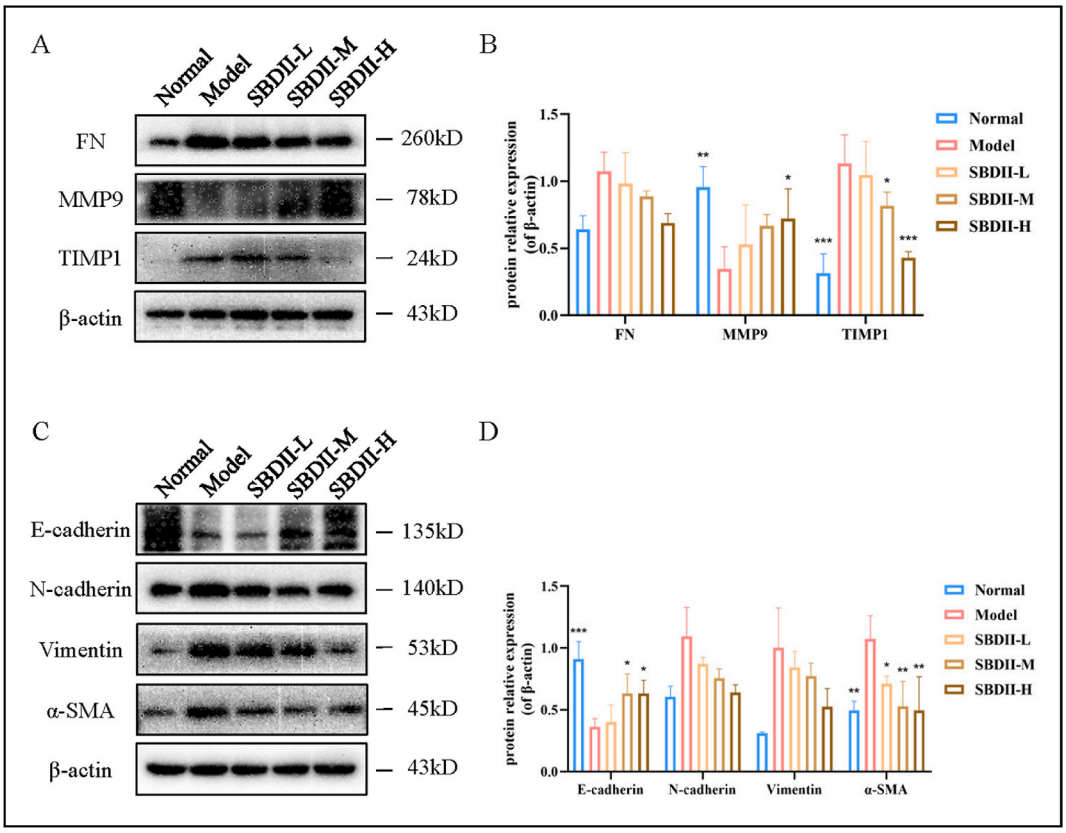

Fig. 8. SBDII treatment improves renal fibrosis in rats with IgAN. (A, C) Rat kidneys were harvested at the end of the experiment, and analyzed to identify the expression of FN, MMP9, TIMP1, E-cadherin, N-cadherin, Vimentin, α-SMA by western blotting. β-actin served as the loading control. For the corresponding full and non-adjusted membranes, see Supplementary Fig. 4 and Supplementary Fig. 5. **(B, D)** Densitometric analysis of FN, MMP9, TIMP1, E-cadherin, N-cadherin, Vimentin, α-SMA expression. Data are expressed as the mean ± SD. $^{*}P < 0.05$, $^{**}P < 0.01$, $^{***}P < 0.001$ (versus model group).

related to IgAN renal fibrosis, indicating the scientific basis for using SBDII to treat IgAN renal fibrosis. The active molecule-target network of SBDII shows that the main active components of SBDII are acacetin, eupatilin, galangin, hispidulin, apigenin, licochalcone E, licoisoflavanone, quercetin, diosmetin, glyasperin D, liquiritigenin, naringenin, etc. Acacetin is a natural plant-derived flavonoid with various biological activities, such as anti-oxidant, anti-inflammatory, and bacteriostatic, and can treat tumor diseases in various ways. Eupatilin, a pharmacologically active flavone derived from Artemisia species, is known to have anti-oxidant and anti-inflammatory activities. Both of them have been reported to attenuate ischemia-reperfusion-induced renal injury in mice and are a promising therapeutic agents against acute ischemia-induced renal damage [22,23]. Galangin is a kind of flavonoid with a wide range of pharmacological activities, including anti-inflammatory, anti-oxidant and anti-fibrosis. An in *vitro* study showed that galangin attenuates oxidative stress-mediated apoptosis in high glucose-induced renal tubular epithelial cells by modulating the renin-angiotensin system and PI3K/AKT/mechanistic target of rapamycin kinase (mTOR) pathway [24]. In addition, previous studies have shown that acacetin, eupatilin, and galangin can be detected in rat plasma after being given to rats by gavage or oral administration, indicating that these active compounds can be absorbed into the blood to play their role [25–27]. Diosmetin, a flavonoid, exists mainly in free or glycoside form in natural plants and edible fruits. An in *vivo* study found that it protects against renal injury in streptozotocin (STZ)-induced diabetic nephropathy mice by modulating the Akt/nuclear factor kappa-B (NF-κB)/inducible nitric oxide synthase (iNOS) signaling pathway [28]. Both can achieve renal protection by regulating the PI3K-Akt signaling pathway, which is consistent with our findings. Hispidulin is also a flavonoid with anti-inflammatory, anti-oxidant, and significant anti-cancer activities [29]. Although there has been no direct report on the treatment of IgAN renal fibrosis with hispidulin, Wu et al. [30] established an in *vitro* model and found that hispidulin can promote podocyte autophagy by increasing the number of autophagic vacuoles to alleviate podocyte damage caused by high glucose. It is suggested that hispidulin can protect the kidneys. Licochalcone E, licoisoflavanone, glyasperin D, and liquiritigenin are all compounds extracted from Glycyrrhiza glabra L. Glycyrrhiza glabra L is one of the most commonly guide drugs for the clinical treatment of IgAN. Previous studies have shown that liquiritigenin can improve renal inflammation by inhibiting renal aquaporin 4 (AQP4)/NF-κB/inhibitor of NF-κB α (IκBα) and NLR family pyrin domain containing 3 (NLRP3) inflammasome activation in potassium oxonate-induced hyperuricemic rats [31]. Apigenin, quercetin, and naringenin are flavonoids and widely exist in nature. Modern pharmacological studies have shown that they have various biological activities, such as

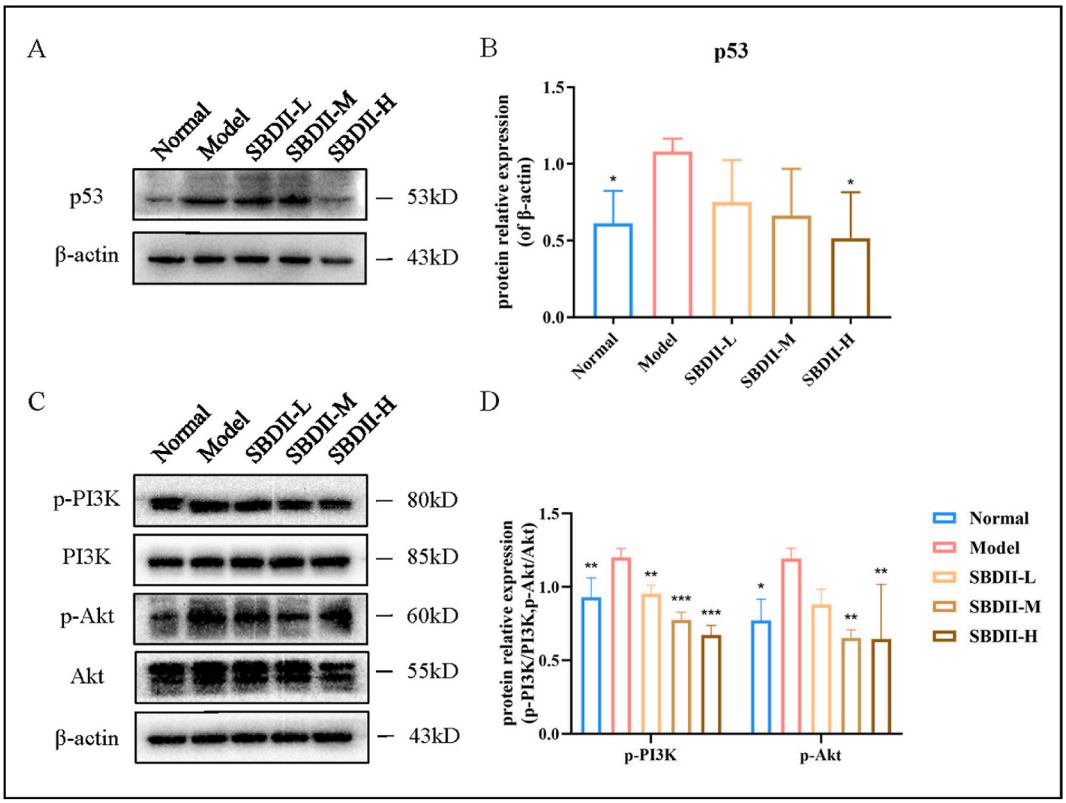

Fig. 9. SBDII treatment reduces p53, p-PI3K and *p*-Akt expressions in rats with IgAN. (A, C) Rat kidneys were harvested at the end of the experiment, and analyzed to identify the expression of p53, p-PI3K, PI3K, *p*-Akt, Akt by western blotting. β-actin served as the loading control. For the corresponding full and non-adjusted membranes, see Supplementary Fig. 6 and Supplementary Fig. 7. **(B, D)** Densitometric analysis of p53, p-PI3K and *p*-Akt expression. Data are expressed as the mean ± SD. $^{*}P < 0.05$, $^{**}P < 0.01$, $^{***}P < 0.001$ (versus model group).

anti-inflammatory, anti-oxidant, and anti-tumor, and play a certain therapeutic role in liver, heart, lung, kidney and nerve diseases [32–34]. It has been suggested that apigenin inhibits renal fibroblast proliferation, differentiation, and function by adenosine 5-monophosphate (AMP)-activated protein kinase (AMPK) activation and reduces extracellular signal-regulated kinase (ERK) 1/2 phosphorylation, thereby inhibiting the development of renal fibrosis [35]. Quercetin has been suggested to delay the progression of glomerulosclerosis and EMT by regulating the transforming growth factor-β (TGF-β) signaling pathway and Hedgehog signaling pathway [36,37]. Combination of naringenin and lisinopril can ameliorate nephropathy in type-1 diabetic rats [38]. Interestingly, quercetin also affects renal function and fibrosis of high-fat diet mice by regulating p53 [39], which is in agreement with our network pharmacology analysis.

The targets with the highest degree in PPI network are TP53, HSP90AA1, GRB2, PIK3R1, SRC, EP300, AKT1 and STAT3. The p53 protein encoded by the TP53 gene is a tumor suppressor, which responds quickly to DNA damage and oncogene activation in cancer cells and normal cells. The activation of p53 may cause cell cycle arrest or apoptosis under various pathophysiological conditions. A study showed that compared with the kidneys of patients with minimal change disease, the expressions of p53, p-STAT3, and α-SMA in the kidneys of patients with IgAN are significantly higher, and there are also tubulointerstitial injury or fibrosis [40]. HSP90AA1 is an important heat shock protein, which can affect the occurrence and development of diabetic nephropathy [41]. GRB2 is one of the important molecules of oxidative stress, and its dysregulation is closely related to renal ischemia-reperfusion injury [42]. SRC is a nonreceptor tyrosine kinase. After SRC inactivation, it can inhibit the activation and proliferation of renal fibroblasts and reduce ECM deposition by inhibiting the activation of TGF-β1, PI3K-Akt and epidermal growth factor receptor (EGFR) signaling pathways and increasing G2/M arrest in epithelial cells [43]. EP300 is a ubiquitously expressed pleiotropic multidomain coactivator involved in apoptosis [44]. PIK3R1 belongs to the PI3Ks protein family and is the regulatory subunit of PI3K. AKT1 is a serine/threonine protein kinase and PI3K's main downstream target for controlling cell proliferation, survival, and cell cycle. STAT3 is considered as a key node in the janus kinase (JAK)-signal transducer and activator of transcription (STAT) signaling pathway and is involved in biological processes such as cell proliferation, differentiation, apoptosis, and immune response. AKT1 and STAT3 activation have been shown to be closely related to the development of IgAN in previous studies [45,46]. These studies further demonstrate that TP53, HSP90AA1, GRB2, PIK3R1, SRC, EP300, AKT1, and STAT3 activities affect renal fibrosis in patients with IgAN.

According to GO and KEGG enrichment analyses, SBDII treatment of IgAN renal fibrosis involves multiple biological processes and signaling pathways, such as PI3K-Akt signaling pathway. PI3K-Akt signaling pathway exists widely in cells, and its interaction with

other pathways is complex. It is one of the important signaling pathways in the body. Both in *vivo* and in *vitro* studies have shown that regulating the PI3K-Akt signaling pathway can significantly improve IgAN renal fibrosis [47,48]. In KEGG pathway enrichment analysis, PI3K is regulated by the upstream Toll-like receptor or JAK-STAT signaling pathway to mediate AKT activation. The activated AKT further affects multiple pathways and multiple biological processes. For example, AKT specifically regulates the transcription and expression of genes such as mTOR, thereby regulating IgAN renal fibrosis; activated AKT also mediates the activation of transcription factors such as MAP kinse-ERK kinase (MEK), ERK, and glycogen synthase kinase (GSK), and plays a role in promoting IgAN renal fibrosis. In addition, NF-κB, p53, B-cell lymphoma 2 (Bcl2), and other factors affect biological processes such as NF-κB signaling pathway, p53 signaling pathway, and apoptosis regulated by AKT (Fig. 10).

Therefore, we speculate that the active components such as acacetin, eupatilin, galangin play important roles in the pharmacological function of SBDII by acting on key molecular targets such as TP53 and regulating PI3K-Akt signaling pathway. In summary, this study has clearly demonstrated the efficacy of SBDII in IgAN renal fibrosis treatment and provides novel ideas for the investigation of the mechanisms underlying its therapeutic effects.

The renal function-related indicators and renal tissue pathological data derived from animal experiments suggest that SBDII possesses a significant protective effect on renal function and fibrosis in IgAN rats. TP53 and PI3K-Akt signaling pathway predicted by network pharmacology are selected for verification. Western blot results show that SBDII downregulates the expression of p53, p-PI3K and *p*-Akt proteins in renal tissues, and at the same time restores the dysregulation of glomerulosclerosis and RIF related proteins. These studies suggest that SBDII targets TP53 and regulates PI3K-Akt signaling pathway to improve IgAN renal fibrosis, which is consistent with the predicted results.

To sum up, this study shows that the active ingredients such as acacetin, eupatilin, and galangin may mediate the therapeutic effects of SBDII in treating IgAN renal fibrosis by targeting TP53 and regulating PI3K-Akt signaling pathway, and some of the targets and pathways predicted by the network pharmacology have been verified in animal experiments. This study suggests the advantages of using SBDII for treating IgAN renal fibrosis by targeting multiple molecular targets and multiple signaling pathways. In the future, we

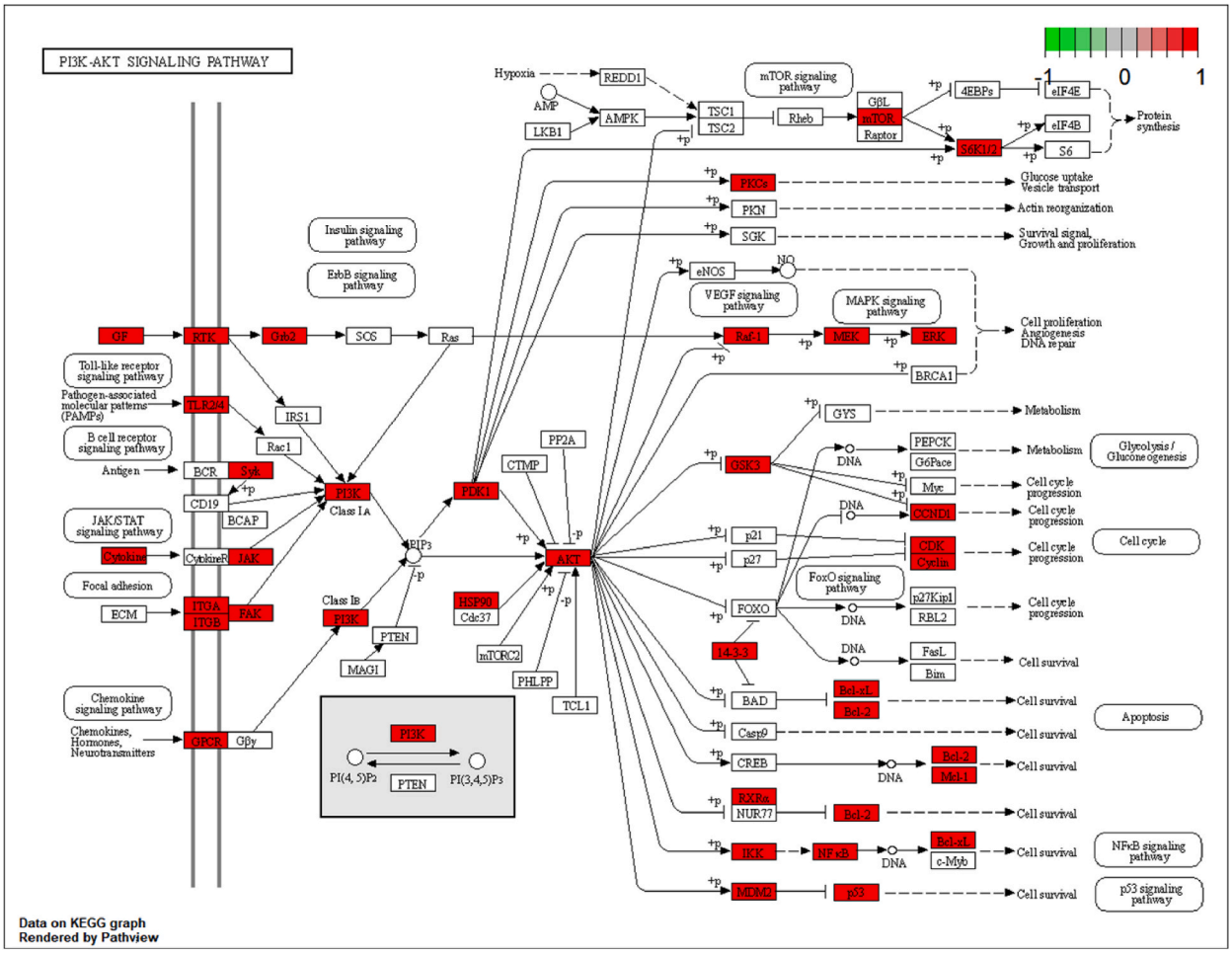

Fig. 10. Schematic diagram of SBDII treating IgAN renal fibrosis by regulating PI3K-Akt signaling pathway. The red nodes belong to 404 potential targets, and the deeper red color, the more important the node plays in SBDII treatment of IgAN renal fibrosis.

will study the anti-IgAN-related biological activities of the active ingredients such as acacetin, eupatilin, galangin and evaluate their contribution to the therapeutic effects of SBDII.

5. Conclusions

This study strongly suggests that SBDII has a therapeutic effect on IgAN renal fibrosis by targeting TP53 and regulating PI3K-Akt signaling pathway, which provides new insights into the mechanism of SBDII in the treatment of IgAN renal fibrosis. In addition, this study also demonstrates the advantages of using TCM for IgAN renal fibrosis treatment.

Ethics approval and consent to participate

The study was approved by the Laboratory Animal Ethics Review Committee of Southern Medical University on May 11, 2016, and the approval ID is L2016054.

Consent for publication

We all agree to publication.

Data availability statement

Data will be made available on request.

Funding

This work was supported by the National Natural Science Foundation of China, China (81673960, 81774212, 81973666), the Natural Science Foundation of Guangdong Province, China (2018030310451, 2018A0303130320, 2019A1515010400, 2019A1515010816), and the Innovation Team and Talents Cultivation Program of the National Administration of Traditional Chinese Medicine, China. (ZYYCXTD-C-202001).

CRediT authorship contribution statement

Huaxi Liu: Data curation, Formal analysis, Methodology, Validation, Writing – original draft. **Weijie Chen:** Validation, Writing – original draft. **Chunyang Tian:** Data curation, Formal analysis, Validation, Writing – original draft. **Yijian Deng:** Validation. **Liangwo Xu:** Validation. **Wenkun Ouyang:** Validation. **Renjie Qiu:** Validation. **Yanting You:** Validation. **Pingping Jiang:** Writing – review & editing. **Lin Zhou:** Writing – review & editing. **Jingru Cheng:** Writing – review & editing. **Hiu Yee Kwan:** Writing – review & editing. **Xiaoshan Zhao:** Conceptualization, Supervision. **Xiaomin Sun:** Conceptualization, Supervision.

Declaration of competing interest

The authors declare that they have no known competing financial interests or personal relationships that could have appeared to influence the work reported in this paper.

Appendix A. Supplementary data

Supplementary data to this article can be found online at https://doi.org/10.1016/j.heliyon.2023.e21997.

Abbreviations

IgAN	IgA nephropathy
SBDII	Shenbing Decoction II
UPLC-MS/MS	ultra-performance liquid chromatography-tandem mass spectrometry
BSA	bovine serum albumin
LPS	lipopolysaccharide
CCL4	carbon tetrachloride
TP53	tumor protein p53
PI3K	phosphatidylinositol 3-kinase
Akt	Akt kinase
ESRF	end-stage renal failure
RIF	renal interstitial fibrosis
ECM	extracellular matrix
EMT	epithelial-mesenchymal transition

TCM	traditional Chinese medicine
SD	Sprague-Dawley
Los	Losartan
SBDII-L	low dose SBDII
SBDII-M	medium dose SBDII
SBDII-H	high dose SBDII
UPCR	urine protein-to-creatinine ratio
Scr	serum creatinine
BUN	blood urea nitrogen
Hyp	Hydroxyproline
H&E	hematoxylin and eosin
FN	fibronectin
MMP9	matrix metallopeptidase 9
TIMP1	TIMP metallopeptidase inhibitor 1
α-SMA	α-smooth muscle actin
HSP90AA1	heat shock protein 90 alpha family class A member 1
GRB2	growth factor receptor bound protein 2
PIK3R1	phosphoinositide-3-kinase regulatory subunit 1
SRC	SRC proto-oncogene, non-receptor tyrosine kinase
EP300	E1A binding protein p300
AKT1	AKT serine/threonine kinase 1
STAT3	signal transducer and activator of transcription 3
BP	biological processes
CC	cellular components
MF	molecular functions
mTOR	mechanistic target of rapamycin kinase
STZ	streptozotocin
NF-κB	nuclear factor kappa-B
iNOS	inducible nitric oxide synthase
AQP4	aquaporin 4
IκBα	inhibitor of NF-κB α
NLRP3	NLR family pyrin domain containing 3
AMPK	adenosine 5-monophosphate (AMP)-activated protein kinase
ERK	extracellular signal-regulated kinase
TGF-β	transforming growth factor-β
EGFR	epidermal growth factor receptor
JAK	janus kinase
STAT	signal transducer and activator of transcription
MEK	MAP kinse-ERK kinase
GSK	glycogen synthase kinase
Bcl2	B-cell lymphoma 2

References

[1] R.J. Wyatt, B.A. Julian, IgA nephropathy, N. Engl. J. Med. 368 (25) (2013) 2402–2414.
[2] A.C. Webster, E.V. Nagler, R.L. Morton, P. Masson, Chronic kidney disease, Lancet (London, England) 389 (10075) (2017) 1238–1252.
[3] M. Perše, Ž. Večerić-Haler, The role of IgA in the pathogenesis of IgA nephropathy, Int. J. Mol. Sci. 20 (24) (2019).
[4] T. Moriyama, K. Tanaka, C. Iwasaki, Y. Oshima, A. Ochi, H. Kataoka, M. Itabashi, T. Takei, K. Uchida, K. Nitta, Prognosis in IgA nephropathy: 30-year analysis of 1,012 patients at a single center in Japan, PLoS One 9 (3) (2014), e91756.
[5] R. Coppo, Treatment of IgA nephropathy: recent advances and prospects, Néphrol. Thérapeutique 14 (Suppl 1) (2018) S13–s21.
[6] M. Wei, X. Zhao, X. Sun, R. Luo, Professor Luo ren's experience in diagnosis and treatment of renal hematuria, Journal of New Chinese Medicine (7) (2008) 10.
[7] M. Wei, X. Sun, X. Zhao, J. Chen, X. Zheng, R. Luo, Effect of shenbing decoction II on oxidative stress in IgA nephropathy patients with pure hematuria, Journal of New Chinese Medicine 43 (1) (2011) 77–79.
[8] M. Wei, X. Zhao, X. Sun, P. Huang, M. Lai, J. Chen, R. Luo, Changes of immune function of erythrocyte of IgA nephropathy of pure hematuria tireated with Shenbing Decoction II, Shandong Med. J. 49 (9) (2009) 19–21.
[9] H. Liu, Y. Deng, W. Chen, L. Xu, B. Xie, P. Xie, G. Luo, W. Zhou, L. Fan, X. Sun, Efficacy and safety of shenbing decoction II for IgA nephropathy simple hematuria, Tradit. Chin. Drug Res. Clin. Pharmacol. 33 (3) (2022) 398–404.
[10] X. Deng, Y. Luo, M. Lu, T. Guan, Y. Li, X. Guo, Unraveling the mechanism of zhibaidihuang decoction against IgA nephropathy using network pharmacology and molecular docking analyses, Tohoku J. Exp. Med. 259 (1) (2022) 37–47.
[11] Z. Fan, J. Chen, Q. Yang, J. He, Network pharmacology and experimental validation to reveal the pharmacological mechanisms of chongcaoyishen decoction against chronic kidney disease, Front. Mol. Biosci. 9 (2022), 847812.
[12] S. Zhou, Z. Ai, W. Li, P. You, C. Wu, L. Li, Y. Hu, Y. Ba, Deciphering the pharmacological mechanisms of taohe-chengqi decoction extract against renal fibrosis through integrating network pharmacology and experimental validation in vitro and in vivo, Front. Pharmacol. 11 (2020) 425.

[13] F. Wang, S. Wang, J. Wang, K. Huang, G. Chen, Y. Peng, C. Liu, Y. Tao, Pharmacological mechanisms of Fuzheng Huayu formula for Aristolochic acid I-induced kidney fibrosis through network pharmacology, Front. Pharmacol. 13 (2022), 1056865.
[14] H. Yuan, X. Wu, X. Wang, C. Yuan, Chinese herbal decoction astragalus and angelica exerts its therapeutic effect on renal interstitial fibrosis through the inhibition of MAPK, PI3K-Akt and TNF signaling pathways, Genes & diseases 9 (2) (2022) 510–521.
[15] L. Yang, Y. Wang, A. Nuerbiye, P. Cheng, J.H. Wang, R. Kasimu, H. Li, Effects of periostracum cicadae on cytokines and apoptosis regulatory proteins in an IgA nephropathy rat model, Int. J. Mol. Sci. 19 (6) (2018).
[16] B.L. Shen, Q.S. Qu, S.Z. Miao, B.L. Liu, R.Y. Liu, D.F. Gu, Study on the effects of regulatory T cells on renal function of IgAN rat model, Eur. Rev. Med. Pharmacol. Sci. 19 (2) (2015) 284–288.
[17] S.N. Peng, H.H. Zeng, A.X. Fu, X.W. Chen, Q.X. Zhu, Effects of rhein on intestinal epithelial tight junction in IgA nephropathy, World J. Gastroenterol. 19 (26) (2013) 4137–4145.
[18] R. Zhu, Y.P. Chen, Y.Y. Deng, R. Zheng, Y.F. Zhong, L. Wang, L.P. Du, Cordyceps cicadae extracts ameliorate renal malfunction in a remnant kidney model, J. Zhejiang Univ. - Sci. B 12 (12) (2011) 1024–1033.
[19] Y.L. Li, L.N. Liu, L. Huang, H.W. An, J.L. Jian, J. Pang, F.N. Lin, W.Q. Yang, J.S. Li, Q. Jiang, et al., Niao du kang mixture increases the expression of mir-129-5p to relieve renal fibrosis, Evid. base Compl. Alternative Med. : eCAM 2020 (2020), 1841890.
[20] H. Liu, Z. Lv, C. Tian, W. Ouyang, Y. Deng, Y. Xiong, X. Zhao, X. Sun, Study on the mechanism of monarch drug of Shenbing Decoction II in the treatment of IgA nephropathy hematuria based on network pharmacology, J. Shenyang Pharm. Univ. 37 (4) (2020) 334–343.
[21] P. Xia, Y. Zhou, W. Li, K. Gao, W. He, W. Sun, Analysis on regularities of recipes for IgA nephropathy based on traditional Chinese medicine inheritance support system, Modernization of Traditional Chinese Medicine and Materia Medica-World Science and Technology 20 (12) (2018) 2255–2261.
[22] A. Shiravi, C. Jalili, G. Vaezi, A. Ghanbari, A. Alvani, Acacetin attenuates renal damage-induced by ischemia-reperfusion with declining apoptosis and oxidative stress in mice, Int. J. Prev. Med. 11 (2020) 22.
[23] E.K. Jeong, H.J. Jang, S.S. Kim, M.Y. Oh, D.H. Lee, D.W. Eom, K.S. Kang, H.C. Kwan, J.Y. Ham, C.S. Park, et al., Protective effect of eupatilin against renal ischemia-reperfusion injury in mice, Transplant. Proc. 47 (3) (2015) 757–762.
[24] J. Liao, B. Liu, K. Chen, S. Hu, Z.Y. Liu, Y.X. Li, Z.M. Yang, M. Zhang, X. Chen, Galangin attenuates oxidative stress-mediated apoptosis in high glucose-induced renal tubular epithelial cells through modulating renin-angiotensin system and PI3K/AKT/mTOR pathway, Toxicol. Res. 10 (3) (2021) 551–560.
[25] J. Yin, Y. Ma, C. Liang, J. Gao, H. Wang, L. Zhang, A systematic study of the metabolites of dietary acacetin in vivo and in vitro based on UHPLC-Q-TOF-MS/MS analysis, J. Agric. Food Chem. 67 (19) (2019) 5530–5543.
[26] X. Wang, J. Ren, S. Zhu, G. Ren, L. Wang, X. Chen, Z. Qiu, C. Zhang, Pharmacokinetics and tissue distribution of eupatilin and its metabolite in rats by an HPLC-MS/MS method, J. Pharmaceut. Biomed. Anal. 159 (2018) 113–118.
[27] W.H. Feng, H.H. Zhang, Y. Zhang, M. Sun, J.L. Niu, Determination of galangin in rat plasma by UPLC and pharmacokinetic study, J. Chromatogr., B: Anal. Technol. Biomed. Life Sci. 998–999 (2015) 26–30.
[28] Y. Jiang, J. Liu, Z. Zhou, K. Liu, C. Liu, Diosmetin attenuates Akt signaling pathway by modulating nuclear factor kappa-light-chain-enhancer of activated B cells (NF-κB)/Inducible nitric oxide synthase (iNOS) in streptozotocin (STZ)-Induced diabetic nephropathy mice, Med. Sci. Mon. Int. Med. J. Exp. Clin. Res. 24 (2018) 7007–7014.
[29] K. Liu, F. Zhao, J. Yan, Z. Xia, D. Jiang, P. Ma, Hispidulin, A promising flavonoid with diverse anti-cancer properties, Life Sci. 259 (2020), 118395.
[30] F. Wu, S. Li, N. Zhang, W. Huang, X. Li, M. Wang, D. Bai, B. Han, Hispidulin alleviates high-glucose-induced podocyte injury by regulating protective autophagy, Biomed. Pharmacother. 104 (2018) 307–314.
[31] L. Hongyan, W. Suling, Z. Weina, Z. Yajie, R. Jie, Antihyperuricemic effect of liquiritigenin in potassium oxonate-induced hyperuricemic rats, Biomed. Pharmacother. 84 (2016) 1930–1936.
[32] S. Malik, K. Suchal, S.I. Khan, J. Bhatia, K. Kishore, A.K. Dinda, D.S. Arya, Apigenin ameliorates streptozotocin-induced diabetic nephropathy in rats via MAPK-NF-κB-TNF-α and TGF-β1-MAPK-fibronectin pathways, Am. J. Physiol. Ren. Physiol. 313 (2) (2017) F414–f422.
[33] B. Ayuda-Durán, S. González-Manzano, A. Miranda-Vizuete, E. Sánchez-Hernández, R.R. M, M. Dueñas, C. Santos-Buelga, A.M. González-Paramás, Exploring target genes involved in the effect of quercetin on the response to oxidative stress in Caenorhabditis elegans, Antioxidants 8 (12) (2019).
[34] Y.Q. Hua, Y. Zeng, J. Xu, X.L. Xu, Naringenin alleviates nonalcoholic steatohepatitis in middle-aged Apoe(-/-)mice: role of SIRT1, Phytomedicine 81 (2021), 153412.
[35] N. Li, Z. Wang, T. Sun, Y. Lei, X. Liu, Z. Li, Apigenin alleviates renal fibroblast activation through AMPK and ERK signaling pathways in vitro, Curr. Pharmaceut. Biotechnol. 21 (11) (2020) 1107–1118.
[36] Y. Liu, E. Dai, J. Yang, Quercetin suppresses glomerulosclerosis and TGF-β signaling in a rat model, Mol. Med. Rep. 19 (6) (2019) 4589–4596.
[37] X. Liu, N. Sun, N. Mo, S. Lu, E. Song, C. Ren, Z. Li, Quercetin inhibits kidney fibrosis and the epithelial to mesenchymal transition of the renal tubular system involving suppression of the Sonic Hedgehog signaling pathway, Food Funct. 10 (6) (2019) 3782–3797.
[38] Y.A. Kulkarni, S.V. Suryavanshi, Combination of naringenin and lisinopril ameliorates nephropathy in type-1 diabetic rats, Endocr., Metab. Immune Disord.: Drug Targets 21 (1) (2021) 173–182.
[39] S.R. Kim, K. Jiang, M. Ogrodnik, X. Chen, X.Y. Zhu, H. Lohmeier, L. Ahmed, H. Tang, T. Tchkonia, L.J. Hickson, et al., Increased renal cellular senescence in murine high-fat diet: effect of the senolytic drug quercetin, Transl. Res. : J. Lab. Clin. Med. 213 (2019) 112–123.
[40] R. Yang, X. Xu, H. Li, J. Chen, X. Xiang, Z. Dong, D. Zhang, p53 induces miR199a-3p to suppress SOCS7 for STAT3 activation and renal fibrosis in UUO, Sci. Rep. 7 (2017), 43409.
[41] Y.A.-O.X. Wang, T. Liu, F. Ma, X. Lu, H. Mao, W. Zhou, L. Yang, P.A.-O. Li, Y.A.-O.X. Zhan, A network pharmacology-based strategy for unveiling the mechanisms of tripterygium wilfordii hook F against diabetic kidney disease, J. Diabetes Res. 2020 (2020), 2421631.
[42] X.R. Zhao, Z. Zhang, M. Gao, L. Li, P.Y. Sun, L.N. Xu, Y. Qi, L.H. Yin, J.Y. Peng, MicroRNA-27a-3p aggravates renal ischemia/reperfusion injury by promoting oxidative stress via targeting growth factor receptor-bound protein 2, Pharmacol. Res. 155 (2020), 104718.
[43] J. Wang, S. Zhuang, Src family kinases in chronic kidney disease, Am. J. Physiol. Ren. Physiol. 313 (3) (2017) F721–F728.
[44] J. Godlewski, B.E. Krazinski, A.E. Kowalczyk, J. Kiewisz, J. Kiezun, P. Kwiatkowski, A. Sliwińska-Jewsiewicka, P.W. Wierzbicki, Z. Kmieć, Expression and prognostic significance of EP300, TP53 and BAX in clear cell renal cell carcinoma, Anticancer Res. 37 (6) (2017) 2927–2937.
[45] N. Guo, S. Liu, L.M. Bow, X. Cui, L. Zhang, S. Xu, S. Lu, J. Tian, The protective effect and mechanism of rapamycin in the rat model of IgA nephropathy, Ren. Fail. 41 (1) (2019) 334–339.
[46] K. Yamada, Z.Q. Huang, M. Raska, C. Reily, J.C. Anderson, H. Suzuki, H. Ueda, Z. Moldoveanu, K. Kiryluk, Y. Suzuki, et al., Inhibition of STAT3 signaling reduces IgA1 autoantigen production in IgA nephropathy, Kidney international reports 2 (6) (2017) 1194–1207.
[47] C. Wang, X. Liu, Z. Ke, Y. Tang, C.C. Li, C.M. Li, Z. Ye, J. Zhang, T. Lou, Mesangial medium from IgA nephropathy patients induces podocyte epithelial-to-mesenchymal transition through activation of the phosphatidyl inositol-3-kinase/Akt signaling pathway, Cell. Physiol. Biochem. : international journal of experimental cellular physiology, biochemistry, and pharmacology 29 (5–6) (2012) 743–752.
[48] F. Dou, Y. Liu, L. Liu, J. Wang, T. Sun, F. Mu, Q. Guo, C. Guo, N. Jia, W. Liu, et al., Aloe-emodin ameliorates renal fibrosis via inhibiting PI3K/Akt/mTOR signaling pathway in vivo and in vitro, Rejuvenation Res. 22 (3) (2019) 218–229.